VIP Nickel Complexes Very Important Paper

How to cite: *Angew. Chem. Int. Ed.* **2021**, *60*, 7077–7081
International Edition: doi.org/10.1002/anie.202011301
German Edition: doi.org/10.1002/ange.202011301

Side-on Coordination in Isostructural Nitrous Oxide and Carbon Dioxide Complexes of Nickel

Braulio M. Puerta Lombardi[+], Chris Gendy[+], Benjamin S. Gelfand, Guy M. Bernard, Roderick E. Wasylishen, Heikki M. Tuononen, and Roland Roesler**

In memory of Professor Suning Wang

Abstract: *A nickel complex incorporating an N_2O ligand with a rare η^2-N,N′-coordination mode was isolated and characterized by X-ray crystallography, as well as by IR and solid-state NMR spectroscopy augmented by ^{15}N-labeling experiments. The isoelectronic nickel CO_2 complex reported for comparison features a very similar solid-state structure. Computational studies revealed that η^2-N_2O binds to nickel slightly stronger than η^2-CO_2 in this case, and comparably to or slightly stronger than η^2-CO_2 to transition metals in general. Comparable transition-state energies for the formation of isomeric η^2-N,N′- and η^2-N,O-complexes, and a negligible activation barrier for the decomposition of the latter likely account for the limited stability of the N_2O complex.*

Among the numerous oxides of nitrogen, nitrous oxide (N_2O) is most intimately intertwined with modern human activities. It figures on the WHO's List of Essential Medicines for use in pain management,[1] and it also has a long history as a recreational drug dubbed "laughing gas".[2] It is used as an oxidant ("nitrous") in racing engines and is a suitable propellant in rockets,[3] as well as in whipped cream and cooking oil canisters. Industrially, N_2O is an important by-product in nitric acid and adipic acid manufacturing.[4] Although industrial pollutants are not to be neglected, natural, enzymatic denitrification processes[5] are the main source of N_2O in the environment and for this reason the gas was proposed to be part of the biosignature of life on exoplanets.[6] The widespread use of nitrogen fertilizers led to an enhancement of denitrification processes and N_2O rose to prominence as a greenhouse gas 300 times more potent than CO_2, and "the dominant ozone-depleting substance emitted in the 21st Century".[7] Although its decomposition into elements is thermodynamically favorable ($\Delta_f H°_{gas}$ 82.1 kJ mol^{-1}), the high activation barrier (250 kJ mol^{-1})[8] associated with this process means that N_2O persists in the atmosphere for an average of 117(8) years.[9] Consequently, interest towards using N_2O as a synthon,[10] as well as towards catalyzing its decomposition into elements has increased in recent years,[11] in turn prompting investigations meant to elucidate the interaction of this prominent small molecule with metals.

N_2O reacts readily with numerous metal complexes and organic substrates, mostly as an oxidant but also as a nitrogen atom donor,[4,10] and can be trapped by frustrated Lewis pairs[12] and N-heterocyclic carbenes (NHCs).[13] Its reactivity involving insertion into M–C and M–H bonds is well documented.[10,14] In contrast to its isoelectronic counterpart CO_2, which has a rich coordination chemistry,[15] N_2O has been generally described as a poor, or exceedingly poor ligand due to its weak σ-donating and π-accepting properties, low polarity, and oxidizing character.[8b,16]

Extensive investigations of ruthenium derivative **A** (Figure 1), which remained for more than three decades the only known metal complex of nitrous oxide, revealed that N_2O coordinated in a linear fashion via the terminal nitrogen

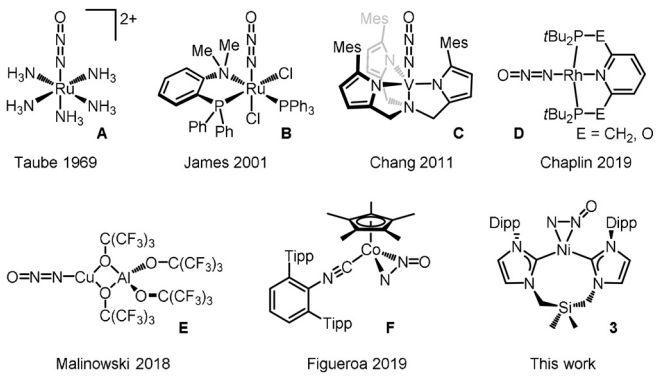

Figure 1. Transition metal complexes of N_2O.

[*] B. M. Puerta Lombardi,[+] Dr. C. Gendy,[+] Dr. B. S. Gelfand, Prof. R. Roesler
Department of Chemistry, University of Calgary
2500 University Drive NW, Calgary, AB, T2N 1N4 (Canada)
E-mail: roesler@ucalgary.ca
Dr. G. M. Bernard, Prof. R. E. Wasylishen
Gunning-Lemieux Chemistry Centre, University of Alberta
11227 Saskatchewan Drive NW, Edmonton, AB, T6G 2G2 (Canada)
Dr. C. Gendy,[+] Prof. H. M. Tuononen
Department of Chemistry, Nanoscience Centre, University of Jyväskylä
P.O. Box 35, FI-40014 Jyväskylä (Finland)
E-mail: heikki.m.tuononen@jyu.fi
[+] These authors contributed equally to this work.
Supporting information and the ORCID identification number(s) for the author(s) of this article can be found under: https://doi.org/10.1002/anie.202011301.

and was a poor ligand susceptible to reduction and displacement.[17] These conclusions were supported by computational studies,[17c,18] the spectroscopic characterization of complex **B**,[19] as well as the NMR characterization of surface-coordinated N_2O.[20] Confirmation of these findings was provided over the last decade by the comprehensive characterization of discrete, end-on bonded complexes **C**, **D** and **E** (Figure 1).[21–23] The rich coordination chemistry of CO_2 suggests that the isoelectronic N_2O molecule should also be able to adopt a bent, *N*,*N*′-side-on coordination mode, which had been probed computationally for surface binding.[24] Linear N_2O bound at the [4Cu:2S] active site of nitrous oxide reductase has been shown to display long, side-on Cu···N contacts.[25] Ultimately, the first η^2-*N*,*N*′-N_2O complex **F**, which was persistent below −25 °C, was recently characterized and the π-basicity of the metal was shown to be key to its isolation.[26]

We reported on a bis(NHC)$_2$Ni^0-$GeCl_2$ complex incorporating a siloxane-linked (NHC)$_2$Ni^0 fragment with a bent L_2M geometry.[27] Computational studies indicated that this fragment featured the frontier orbitals necessary for efficient η^2-interactions with π-acidic ligands.[18c,28] Thus, we hypothesized that a bis(NHC)$_2$ supported Ni^0 would be an excellent candidate for stabilizing side-on, η^2-N_2O complexes, especially taking into account the resilience of NHC ligands to oxidation. Design of ligand **1**, incorporating a shorter silane linker, aimed to impose a narrow C_{NHC}-Ni-C_{NHC} angle and increase the π-basicity of the metal.[29] This allowed us to characterize analogous η^2-bound Ni^0 complexes of N_2O and CO_2 and to assess the relative binding ability of the two ligands for the first time.

Prepared by deprotonation of its bis(imidazolium) precursor, ligand **1** reacted with Ni(cod)$_2$ to yield (**1**)Ni(η^2-cod), **2** (Scheme 1). Solution ^{1}H NMR analysis of **2** revealed a broad, complex spectrum denoting C_1 symmetry, reflected in the ^{13}C NMR spectrum by the presence of two resonances for the coordinated carbene carbons (200.4 and 208.4 ppm). Reduced conformational fluxionality in complexes containing bis(NHC)Ni fragments was shown to lead to broad, poorly resolved resonances in the solution NMR spectra, as well as lowering of the expected time-averaged symmetry.[27] An X-ray diffraction experiment on **2** confirmed chelation of the ligand to Ni in a bent geometry (C1-Ni1-C8 107.9(1)°) (Figure S28) and the η^2-coordination of 1,5-cyclooctadiene.

In solution, complex **2** reacted with 1 atm of N_2O at room temperature to yield **3**, which was isolated as a yellow crystalline solid. The low solubility of **3** precluded its characterization in solution. As a solid, it can be stored for months at −78 °C and handled at room temperature in vacuum or under an inert atmosphere, but partial decomposition is apparent after 12 hours at room temperature (by IR). Heating to 70 °C in THF leads to dissolution upon N_2 development (Figure S3). The ^{13}C CP-MAS NMR spectrum of **3** (Figure S19) features two resonances corresponding to the coordinated carbene carbons at 183.7 and 192.5 ppm, similar to the values measured in solution for **2**.

The ^{15}N CP-MAS NMR resonances for bound N_2O in an isotopically enriched sample of **3** were observed at 365 and 312 ppm (Figure 2), corresponding to the central and terminal

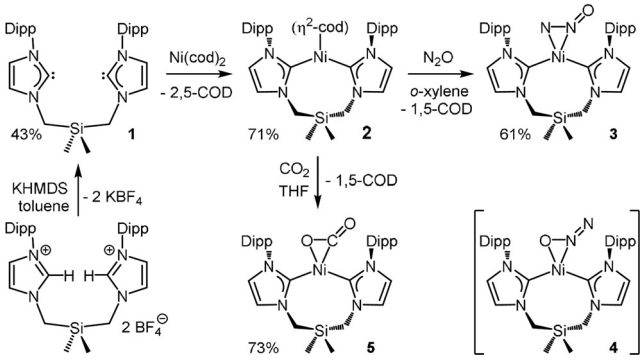

Scheme 1. Synthesis of compounds **1**–**3** and **5**, and the postulated, fleeting η^2-*N*,*O*-isomer **4**. Dipp = 2,6-diisopropylphenyl.

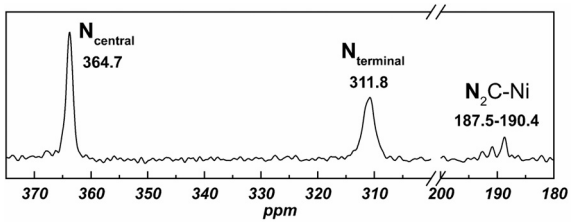

Figure 2. ^{15}N CP-MAS NMR spectrum of **3** containing 33 % $^{15}N_2O$, the latter prepared using an original method (see Supporting Information).

nitrogen atoms in N_2O, respectively (vs. the gas phase computed values of 395 and 313 ppm). These values are significantly deshielded compared to those observed in the κ^1-*N*-N_2O and the η^2-*N*,*N*′-N_2O complexes, as well as those for free N_2O (Table 1). Resonances corresponding to the naturally abundant nitrogen atoms in the imidazole rings appear between 187.5–190.4 ppm, matching literature data for NHC ligands.[30] Infrared spectroscopy suggests that N_2O is side-on, η^2-*N*,*N*′-coordinated in **3**. The observed ν_{NN} stretching and ν_{NNO} bending vibrations (Figure 3) at 1533 and 1138 cm^{-1}, respectively (vs. the gas phase computed values of 1725 and 1243 cm^{-1}, and the experimental values for **F** of 1624 and 1131 cm^{-1}) shift to lower frequencies (1495 and 1121 cm^{-1}) in ^{15}N-enriched samples of **3**. The ν_{NN} stretching vibration measured in **3** is the lowest value observed in N_2O metal complexes, both κ^1-*N*-N_2O (2234–2303 cm^{-1} for ν_{NN} and 1150–1337 cm^{-1} for ν_{NO} in **A**–**E**) and η^2-*N*,*N*′-N_2O (1624 cm^{-1} for ν_{NN} and 1131 cm^{-1} for ν_{NNO} in **F**), in agreement with the high π-basicity of the (**1**)Ni^0 fragment and its strong interaction with the π* system of N_2O.

X-ray crystallography revealed for **3** the expected, bent (**1**)Ni fragment (∡CNC 104.47(13)°) with the side-on, η^2-*N*,*N*′-coordinated N_2O ligand completing the coordination

Table 1: Selected ^{15}N NMR resonances for free and bound N_2O.

Cpd.	N_2O[26]	**B**[19]	**D**[a],[22]	**D**[b],[22]	**F**[26]	**3**	**3**[c]
Solv.	tol-d_8	CD_2Cl_2	DFB[d]	DFB[d]	tol-d_8	solid	gas
δN_{term}	135	126	109	103	159	312	313
δN_{cent}	218		245	246	309	365	395

[a] E = CH_2. [b] E = O. [c] Computed. [d] DFB = 1,2-$F_2C_6H_4$.

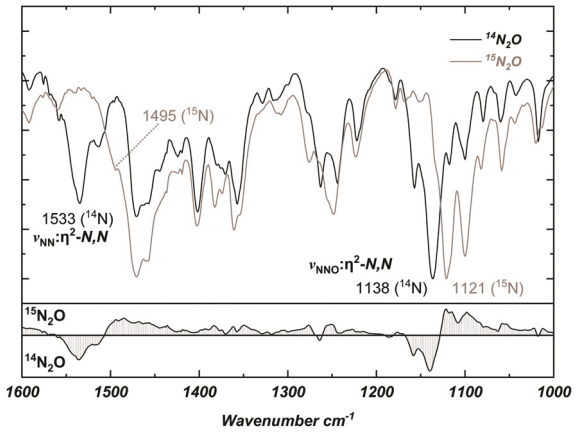

Figure 3. Overlaid FT-IR spectra for **3** and **3**-($^{15}N_2O$) (99% isotopically enriched) with spectral difference below.

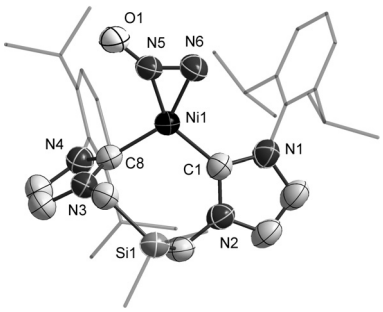

Figure 4. Solid-state structure of one of the two independent molecules of **3** with 50% thermal ellipsoids, and hydrogen atoms omitted. Selected bond lengths [Å] and angles [°] with [calculated values]: N5–N6 1.225(4) [1.210], N5–O1 1.276(4) [1.239], Ni1–N5 1.803(3) [1.821], Ni–N6 1.926(3) [1.910], Ni1–C1 1.901(3) [1.934], Ni1–C8 1.893(3) [1.919]; N5-N6-O1 134.7(3) [138.4], C1-Ni1-C8 104.47(13) [107.7].

sphere of nickel (Figure 4). The metric parameters characterizing the N_2O moiety (N5–N6 1.225(4) Å and N5–O1 1.276(4) Å) are consistent with the calculated values and compare well with the N–N bond length measured in **F** (1.212(8) Å). The dihedral angle formed by the N_2O and $C_{NHC}NiC_{NHC}$ planes measures only 8.4(3)°.

Aiming to provide a comparison for **3**, its CO_2 analog **5** was prepared by reaction of **2** with 1 atm of CO_2 in THF. The product was stable under an inert atmosphere and did not dissolve in hydrocarbon or ethereal solvents. The solid-state ^{13}C NMR spectrum of **5** (Figure S21) is very similar to the spectrum of **3**, featuring two carbene resonances (188.2 and 192.2 ppm) and a resonance corresponding to the CO_2 ligand (167.3 ppm). A characteristic ν_{CO} stretching vibration is observed in the IR spectrum of **5** at 1695 cm^{-1} (vs. the gas phase computed value of 1855 cm^{-1}). The solid-state structure of **5** (Figure 5) is very similar to that of **3**. The bond angles in the coordinated CO_2 and N_2O match closely ($\sphericalangle$NNO 134.7(3)° in **3** vs. $\sphericalangle$OCO 135.0(2)° in **5**) but differences are apparent in the bond distances to their terminal atoms (N5–O1 1.275(3) Å in **3** vs. C35–O2 1.217(3) Å in **5**).

A DFT comparison of the binding energies of L in (**1**)Ni(L) (with $\Delta G°$ in parenthesis) yielded values of 87 (33) and 110 (56) kJ mol^{-1} for L = CO_2 and N_2O, respectively,

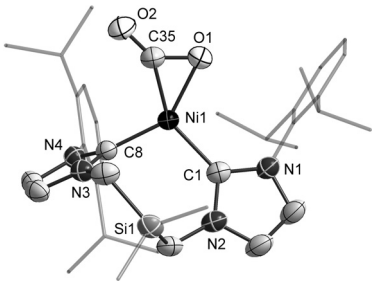

Figure 5. Solid-state structure of **5** with 50% thermal ellipsoids, and hydrogen atoms omitted. Selected bond lengths [Å] and angles [°] with [calculated values]: O1–C35 1.283(4) [1.264], C35–O2 1.218(4) [1.206], Ni1–O1 1.949(2) [1.937], Ni–C35 1.828(3) [1.839], Ni1–C1 1.973(3) [1.964], Ni1–C8 1.866(2) [1.856]; O1-C35-O2 134.6(3) [137.5], C1-Ni1-C8 106.95(10) [109.4].

while for a hypothetical complex of (**1**)Ni with the classic π-acceptor ethylene, the energies are even greater, at 129 (74) kJ mol^{-1}. Furthermore, an energy decomposition analysis with ETS-NOCV revealed that the instantaneous interaction energies of L in (**1**)Ni(L) follow a similar trend, largely owing to the significantly stronger orbital interactions (in parathesis): −401 (−643) and −415 (−709) kJ mol^{-1} for L = CO_2 and N_2O, respectively. The total orbital interaction term can further be decomposed using NOCV, showing a dominant contribution (83% for **3** and 84% for **5**) involving donation from the metal to the π* system of the ligand. Taken as a whole, the results of DFT calculations indicate that N_2O binds to (**1**)Ni^0 slightly stronger than CO_2 due to stronger orbital interactions in **3**. To probe whether the observed energetic trend is more general, the equilibrium TM-CO_2 + N_2O ⇌ TM-N_2O + CO_2 (TM = transition metal fragment) was analyzed computationally for 12 crystallographically characterized η^2-*C*,*O*-CO_2 complexes and their hypothetical N_2O analogues. The data (Table S2) showed stronger binding for N_2O in 9 systems (up to 26 kJ mol^{-1}) demonstrating that when bound in η^2-fashion, N_2O is a comparable or slightly better π-acceptor than CO_2. However, it needs to be stressed that N_2O is oxidizing whereas CO_2 is not, for which reason the increased binding energy in the hypothetical N_2O systems considered above is unlikely to stabilize η^2-*N*,*N*-N_2O complexes over metal or ligand oxidation.

The energy landscape for the formation of **3** from (**1**)Ni^0 and N_2O was also probed with computational methods (Figure S31). The results revealed that the formation of **3** involves a modest barrier ($\Delta G^{\ddagger}$ = 38 kJ mol^{-1}), with $\Delta G°$ = −56 kJ mol^{-1}. The formation of the η^2-*O*,*N*-N_2O isomer, **4**, though not observed experimentally, was found to involve a greater barrier ($\Delta G^{\ddagger}$ = 70 kJ mol^{-1}) and a minute $\Delta G°$ of −2 kJ mol^{-1}. However, **4** appears to be a metastable species and readily converts to (**1**)NiO(N_2) almost without a barrier. Barrierless decomposition of η^2-*O*,*N*-N_2O bound to iron has been investigated computationally and matched experimental observations.[31] Thus, at a relative energy of −63 kJ mol^{-1}, (**1**)NiO(N_2) represents the lowest energy point on the potential energy surface and confirms that metal-oxo formation is thermodynamically favored over η^2-*N*,*N*-N_2O complex formation, albeit only by 7 kJ mol^{-1}. As suggested by the

calculated energy landscape, **3**, unlike **5**, is a kinetic, not a thermodynamic, product, in agreement with its limited stability. Similarly, decomposition of **F** was reported to proceed via formation of a reactive metal-oxo species and transfer of oxygen to the ancillary isocyanide ligand.[26]

To summarize, employing the π-basic fragment (**1**)Ni, we isolated **3** by reaction of **2** with N_2O. The rare η^2-*N*,*N*′-coordination mode of the N_2O ligand in **3** was proved by single-crystal X-ray crystallography, as well as ^{15}N CP-MAS NMR and IR spectroscopy aided by ^{15}N isotopic enrichment. The isostructural, η^2-CO_2 complex **5** was also synthesized, allowing a direct comparison of the metal binding properties of the two isoelectronic small molecules of environmental relevance. Computational studies indicate that π-acceptance is the main contributor to N_2O binding in **3**, and place the η^2-*N*,*N*′-metal binding ability of this ligand to the (**1**)Ni fragment in-between that of CO_2 and ethylene. In general, the η^2-*N*,*N*′-binding ability of N_2O to transition metals is found to be comparable to, or slightly better than that of CO_2. This demonstrates that the need for a strongly π-basic metal fragment comes not so much from the frequently invoked "poor σ-donating and π-accepting properties" of N_2O, but from the need to stabilize η^2-*N*,*N*′-coordination over the thermodynamically more favorable metal-oxo formation. The well-known oxidizing character of N_2O may be mostly, if not entirely responsible for the scarcity of η^2-metal complexes employing this ligand, and more of such complexes are expected to be in reach in designs featuring the right balance of π-basicity and resilience to oxidation at the metal center and associated ligands.

Acknowledgements

Financial support was provided by the Universities of Calgary, Jyväskylä, and Alberta, as well as the NSERC of Canada in the form of Discovery Grants #2019-07195 to R.R. and #2019-06816 to R.E.W. The project received funding from the European Research Council under the EU's Horizon 2020 programme (grant #772510 to H.M.T). R.E.W. acknowledges the CFI and the Government of Alberta for NMR Facilities support. Computational resources were provided by the Finnish Grid and Cloud Infrastructure (persistent identifier urn:nbn:fi:research-infras-2016072533) and the University of Calgary.

Conflict of interest

The authors declare no conflict of interest.

Keywords: back bonding · carbon dioxide · N-heterocyclic carbenes · nickel · nitrous oxide

[1] World Health Organization. World Health Organization model list of essential medicines: 21st list 2019. **2019** Geneva: World Health Organization.
[2] M. Laing, *S. Afr. J. Sci.* **2003**, *99*, 109 – 114.
[3] V. Zakirov, M. Sweeting, T. Lawrence, J. Sellers, *Acta Astronautica* **2001**, *48*, 353 – 362.
[4] V. N. Parmon, G. I. Panov, A. Uriarte, A. S. Noskov, *Catal. Today* **2005**, *100*, 115 – 131.
[5] a) N. Lehnert, H. T. Dong, J. B. Harland, A. P. Hunt, C. J. White, *Nat. Rev. Chem.* **2018**, *2*, 278 – 289.
[6] a) J. L. Grenfell, *Phys. Rep.* **2017**, *713*, 1 – 17.
[7] A. R. Ravishankara, J. S. Daniel, R. W. Portmann, *Science* **2009**, *326*, 123 – 125.
[8] a) A. H. H. Chang, D. R. Yarkony, *J. Chem. Phys.* **1993**, *99*, 6824 – 6831; b) W. C. Trogler, *Coord. Chem. Rev.* **1999**, *187*, 303 – 327.
[9] M. J. Prather, J. Hsu, N. M. DeLuca, C. H. Jackman, L. D. Oman, A. R. Douglass, E. L. Fleming, S. E. Strahan, S. D. Steenrod, O. A. Søvde, I. S. A. Isaksen, L. Froidevaux, B. Funke, *J. Geophys. Res. Atmos.* **2015**, *120*, 5693 – 5705.
[10] K. Severin, *Chem. Soc. Rev.* **2015**, *44*, 6375 – 6386.
[11] M. Konsolakis, *ACS Catal.* **2015**, *5*, 6397 – 6421.
[12] a) E. Otten, R. C. Neu, D. W. Stephan, *J. Am. Chem. Soc.* **2009**, *131*, 9918 – 9919; b) R. C. Neu, E. Otten, A. Lough, D. W. Stephan, *Chem. Sci.* **2011**, *2*, 170 – 176; c) M. J. Kelly, J. Gilbert, R. Tirfoin, S. Aldridge, *Angew. Chem. Int. Ed.* **2013**, *52*, 14094 – 14097; *Angew. Chem.* **2013**, *125*, 14344 – 14347.
[13] a) A. G. Tskhovrebov, E. Solari, M. D. Wodrich, R. Scopelliti, K. Severin, *Angew. Chem. Int. Ed.* **2012**, *51*, 232 – 234; *Angew. Chem.* **2012**, *124*, 236 – 238; b) A. G. Tskhovrebov, B. Vuichoud, E. Solari, R. Scopelliti, K. Severin, *J. Am. Chem. Soc.* **2013**, *135*, 9486 – 9492.
[14] a) G. A. Vaughan, P. B. Rupert, G. L. Hillhouse, *J. Am. Chem. Soc.* **1987**, *109*, 5538 – 5539; b) G. A. Vaughan, C. D. Sofield, G. L. Hillhouse, A. L. Rheingold, *J. Am. Chem. Soc.* **1989**, *111*, 5491 – 5493.
[15] a) A. Pastor, A. Montilla, F. Galindo, *Adv. Organomet. Chem.* **2017**, *68*, 1 – 91; b) A. Paparo, J. Okuda, *Coord. Chem. Rev.* **2017**, *334*, 136 – 149.
[16] W. B. Tolman, *Angew. Chem. Int. Ed.* **2010**, *49*, 1018 – 1024; *Angew. Chem.* **2010**, *122*, 1034 – 1041.
[17] a) J. N. Armor, H. Taube, *J. Am. Chem. Soc.* **1969**, *91*, 6874 – 6876; b) F. Bottomley, W. V. F. Brooks, *Inorg. Chem.* **1977**, *16*, 501 – 502; c) F. Paulat, T. Kuschel, C. Näther, V. K. K. Praneeth, O. Sander, N. Lehnert, *Inorg. Chem.* **2004**, *43*, 6979 – 6994.
[18] a) D. F.-T. Tuan, R. Hoffmann, *Inorg. Chem.* **1985**, *24*, 871 – 876; b) H. Yu, G. Jia, Z. Lin, *Organometallics* **2008**, *27*, 3825 – 3833; c) J. G. Andino, K. G. Caulton, *J. Am. Chem. Soc.* **2011**, *133*, 12576 – 12576.
[19] C. B. Pamplin, E. S. F. Ma, N. Safari, S. J. Rettig, B. R. James, *J. Am. Chem. Soc.* **2001**, *123*, 8596 – 8597.
[20] a) S. Hu, T. M. Apple, *J. Catal.* **1996**, *158*, 199 – 204; b) V. M. Mastikhin, I. L. Mudrakovsky, S. V. Filimonova, *Chem. Phys. Lett.* **1988**, *149*, 175 – 179; c) V. M. Mastikhin, I. L. Mudrakovsky, S. V. Filimonova, *Zeolites* **1990**, *10*, 593 – 597.
[21] N. A. Piro, M. F. Lichterman, W. H. Harman, C. J. Chang, *J. Am. Chem. Soc.* **2011**, *133*, 2108 – 2111.
[22] M. R. Gyton, B. Leforestier, A. B. Chaplin, *Angew. Chem. Int. Ed.* **2019**, *58*, 15295 – 15298; *Angew. Chem.* **2019**, *131*, 15439 – 15442.
[23] V. Zhuravlev, P. J. Malinowski, *Angew. Chem. Int. Ed.* **2018**, *57*, 11697 – 11700; *Angew. Chem.* **2018**, *130*, 11871 – 11874.
[24] a) C.-L. Hu, Y. Chen, J.-Q. Li, Y.-F. Zhang, *Chem. Phys. Lett.* **2007**, *438*, 213 – 217; b) A. Heyden, B. Peters, A. T. Bell, F. J. Keil, *J. Phys. Chem. B* **2005**, *109*, 1857 – 1873.
[25] A. Pomowski, W. G. Zumft, P. M. H. Kroneck, O. Einsle, *Nature* **2011**, *477*, 234 – 237.
[26] C. C. Mokhtarzadeh, C. Chan, C. E. Moore, A. L. Rheingold, J. S. Figueroa, *J. Am. Chem. Soc.* **2019**, *141*, 15003 – 15007.
[27] C. Gendy, A. Mansikkamäki, J. Valjus, J. Heidebrecht, P. C.-Y. Hui, G. M. Bernard, H. M. Tuononen, R. E. Wasylishen, V. K.

Michaelis, R. Roesler, *Angew. Chem. Int. Ed.* **2019**, *58*, 154 – 158; *Angew. Chem.* **2019**, *131*, 160 – 164.
[28] a) T. Ziegler, *Inorg. Chem.* **1985**, *24*, 1547 – 1552; b) L. P. Wolters, F. M. Bickelhaupt in *Structure and Bonding* (Eds.: O. Eisenstein, S. Macgregor), Springer, Berlin, **2014**.
[29] a) C. Massera, G. Frenking, *Organometallics* **2003**, *22*, 2758 – 2765; b) F. Hering, J. Nitsch, U. Paul, A. Steffen, F. M. Bickelhaupt, U. Radius, *Chem. Sci.* **2015**, *6*, 1426 – 1432.
[30] A. J. Arduengo, R. L. Harlow, M. Kline, *J. Am. Chem. Soc.* **1991**, *113*, 361 – 363.
[31] a) P. B. Armentrout, L. F. Halle, J. L. Beauchamp, *J. Chem. Phys.* **1982**, *76*, 2449 – 2457; b) L. Zhao, Y. Wang, W. Guo, H. Shan, X. Lu, T. Yang, *J. Phys. Chem. A* **2008**, *112*, 5676 – 5683.

Manuscript received: August 19, 2020
Revised manuscript received: October 5, 2020
Accepted manuscript online: October 27, 2020
Version of record online: February 17, 2021

